QIRT10 http://dx.doi.org/10.21611/qirt.2010.009
10th International Conference on Quantitative InfraRed Thermography
July 27-30, 2010, Québec (Canada)

Simple possibilities of thermal diffusivity estimation for small-sized samples, with a laser pulse heating and infrared cameras

by V. Ayvazyan*, J.-C. Batsale*, C. Pradere*

*TREFLE laboratory UMR 8508 : CNRS-ENSAM-UB1, Esplanade des Arts et Métiers, 33405 Talence.
vigen.ayvazyan@bordeaux.ensam.fr , christophe.pradere@bordeaux.ensam.fr, jean-christophe.batsale@bordeaux.ensam.fr

Abstract

The laser pulse heating is nowadays a very convenient and cheap way for the extension of metrological possibilities of infrared cameras. Laser diodes and simple optical systems, such as dichroic mirors (see Fig. 1), offer large possibilities to implement front face analysis of homogeneous solids. The front face temperature field can be processed from the knowledge of suitable analytical expressions which main characteristics will be presented here.

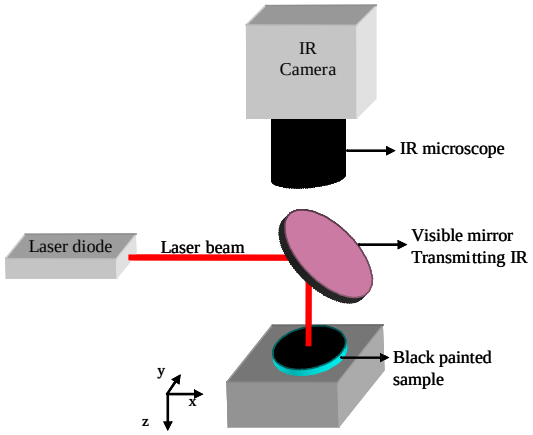

Fig. 1. *Optical devices for the measurement of thermal diffusivities with an infrared camera at small scales (the diameter of the laser beam is lower than one millimeter)*

1. Analytical solution

The analytical expression of the temperature response field of a point source heat pulse, imposed on the front face of a semi-infinite orthotropic solid at *x=y=z=0* yields:

$$T(x,y,z,t) = \frac{Q}{\rho c}\frac{\exp\left(x^2/(4a_x t)\right)}{\sqrt{\pi a_x t}}\frac{\exp\left(y^2/(4a_y t)\right)}{\sqrt{\pi a_y t}}\frac{\exp\left(z^2/(4a_z t)\right)}{\sqrt{\pi a_z t}} \qquad (1)$$

with:

a_x, a_y, a_z : thermal diffusivities versus *x,y,z* direction ($m^2 s^{-1}$)

Q : Energy of the pulse point source (*J*)

ρc : volumic heat capacity ($Jkg^{-1}K^{-1}$)

Such expression is separable and can be expressed as a product of 3 responses related each other to a 1D diffusion behaviour. It is very convenient for the estimation of thermophysical properties such as a_x, a_y, a_z related to the thermal diffusivities following *x, y* and *z* directions.

In the past, from these considerations, several methods such as hot wire, hot plane or hot disk (see [1], [2]) have been developed with solid thin film or thin wire heating and measuring at the same time and the same place as the probe, the temperature response (with the same resistive probe or an additional thermocouple). The drawback of these methods is related to the inertia of the measurement device and the thermal contact resistance between the probe and the substrate. Generally, such contact methods do not allow the investigation of small-sized samples and the single located temperature information must be strongly related to the shape of the heating area (plane, wire or point).

The transposition of such methods to the use of laser heating and non contact infrared cameras presents several advantages linked to the absence of inertia related to heating and temperature measurement. Even if the absolute level of the heat flux and temperature are not easily accessible, the space averaging possibilities of the temperature frames offer 3 estimation possibilities in a single experiment.

http://dx.doi.org/10.21611/qirt.2010.009
10th International Conference on Quantitative InfraRed Thermography

2. Processing the front face temperature field

One way to process the front surface temperature field (*T(x,y,z=0,t)*) is to consider the Fourier cosine transform on the space variables (x,y) (see [3] , [4]), such as:

$$\theta(\alpha_n, \beta_m, z=0,t) = \int_0^L \int_0^l T(x,y,z=0,t)\cos(\alpha_n x)\cos(\beta_m y)dxdy \qquad (2)$$

with *L* and *l* are the lateral size of the sample and $\alpha_n = n\pi / L$ and $\beta_m = m\pi / l$ are dicrete eigenvalues.

The Fourier transform method can be applied if the heating is a pulse but not necessary a point source. In the case of a point source, the short time approximation (when *l* and *L* are assumed to be large or infinite) of the Fourier transform of expression (1) is:

$$\theta(\alpha_n, \beta_m, z=0,t) = \frac{Q}{\rho c}\exp\left(-a_x {\alpha_n}^2 t\right)\exp\left(-a_y {\beta_m}^2 t\right)\left(1/\sqrt{\pi a_z t}\right) \qquad (3)$$

This last expression demonstrates that from a single point source experiment the consideration of marginal space averaging (from $\alpha_n = 0$ or $\beta_m = 0$ in Fourier space) such as:

$$\left\langle \left\langle T(z=0,t)\right\rangle_x \right\rangle_y = \frac{1}{lL}\int_0^L \int_0^l T(x,y,z=0,t)dxdy\,; \qquad \left\langle T(y,z=0,t)\right\rangle_x = \frac{1}{L}\int_0^L T(x,y,z=0,t)\,dx \qquad (4)$$

will give 3 different transient behaviours as follows:

$$\left\langle \left\langle T(z=0,t)\right\rangle_x \right\rangle_y = \frac{Q}{\rho c L l}\frac{1}{\sqrt{a_z \pi t}}, \quad (5.a)$$

$$\left\langle T(y,z=0,t)\right\rangle_x = \frac{Q}{\rho c L}\frac{1}{\sqrt{a_z \pi t}}\frac{\exp\left(-y^2/(4a_y t)\right)}{\sqrt{a_y \pi t}}, \quad (5.b)$$

$$\left\langle T(x,z=0,t)\right\rangle_y = \frac{Q}{\rho c l}\frac{1}{\sqrt{a_z \pi t}}\frac{\exp\left(-x^2/(4a_x t)\right)}{\sqrt{a_x \pi t}} \qquad (5.c)$$

(these expressions are obtained from equation (3) after inverse Fourier transform)

Such behaviours allow considering accurately the different diffusion regimes in 1D, 2D or 3D mode, and give a way to verify the experimental behaviours. The previous expressions (5) will be illustrated through several examples of experiments in the following sections.

3. Laser pulse heating setup

3.1 Study of spatial average value of temperature in *x* and *y* directions (see (5.a))

In this experiment, we assume that the thermal heat losses need not to be taken in consideration, as they have low influence at small scales.

The sample under study is a Silica-Phenolic composite with a thickness of 6 mm and *L=l=20* mm, used for thermal protection systems, such as thermal shields on space shuttles, it's transverse thermal diffusivity is about $3.5*10^{-7}$ $m^2.s^{-1}$. The sample's surface is covered with a thin black paint in order to have the same absorption all over the surface and decrease reflections on it.

The heat source is a 1 W power laser diode, 830 nm wavelength, which illuminates the sample's surface during about 360 ms. Optical lens is used to focus the laser beam and a dichroic mirror to guide the laser beam onto the sample. The dichroic mirror is reflective for visible radiation (between 400 nm and 1000 nm wavelengths) and is transparent for IR radiation (95% transmission between 2 and 5 µm wavelengths). The emitted IR radiation from the heated sample goes through dichroic mirror and is measured by an IR camera (*FLIR ATS Titanium* InSb camera with 320*256 pixels detector and 1.9-5.2 µm wavelength detection band, coupled with a microscope IR objective). It allows to consider the front face temperature variation of the sample on Fig. 2.

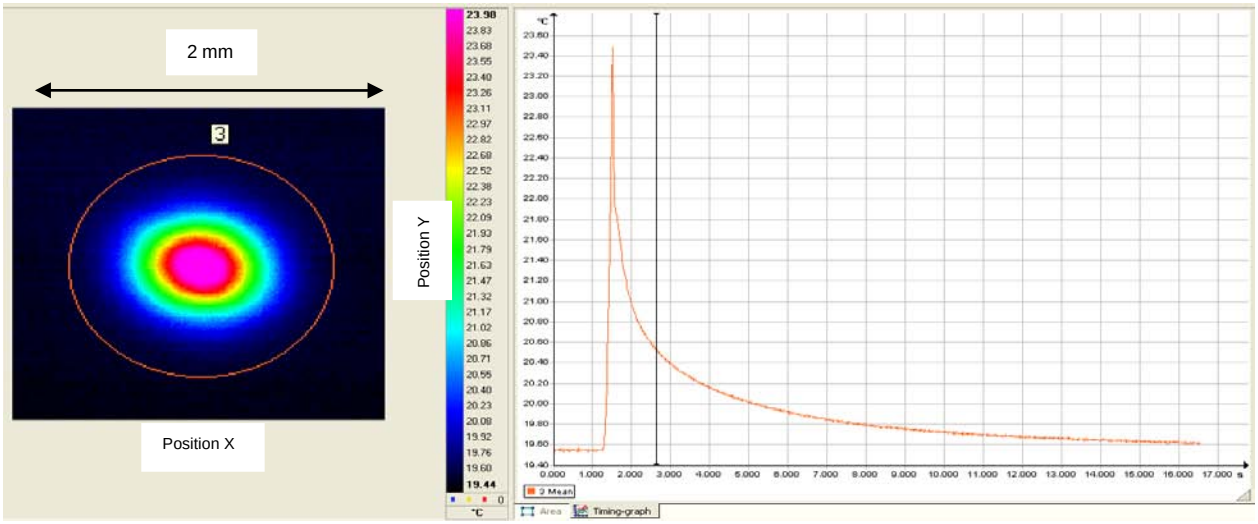

Fig. 2. *Average temperature evolution of sample's surface for the pixels inside the circle (1 pixel corresponds approximately to 30 µm on the sample). The peak observed on the graph corresponds to the heat pulse, which illuminates the sample* during about 360 ms *at ½ W. The average temperature increase inside the circle is less than 5 °C. The integration time is equal to 500 µs and camera's acquisition frequency is 50 Hz. About 17 s are needed to perform the experiment, 800 IR images are recorded*

From the measured IR images, resulting temperature fields are represented Fig.3.

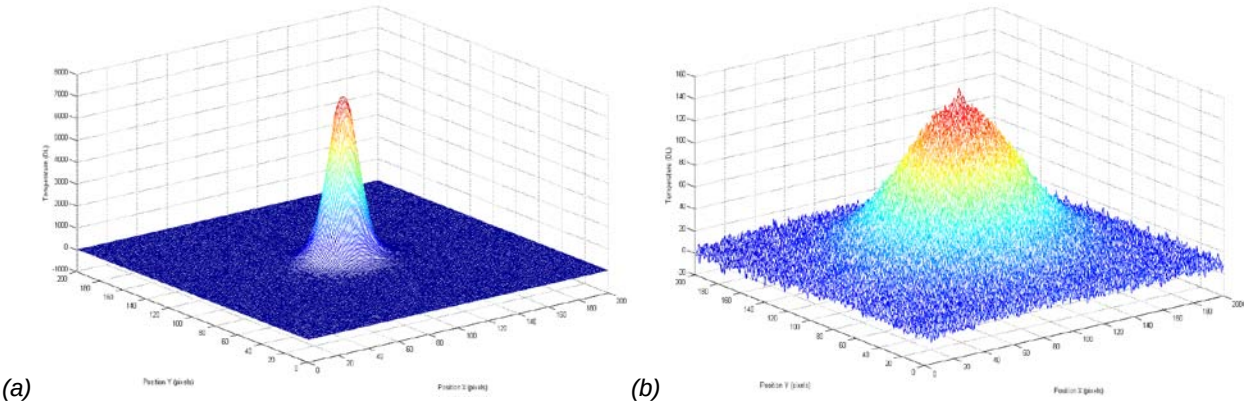

(a) *(b)*

Fig. 3. *Measured temperature fields: (a) just after heat pulse (b) during themal relaxation, semi-infinite behaviour*

From these measurements, the logarithm of spatial average value (in *x* and *y* directions) of the temperature is plotted versus logaritm of time Fig. 4. The -1/2 slope correspondig to the semi-infinite behaviour is well observed.

http://dx.doi.org/10.21611/qirt.2010.009
10th International Conference on Quantitative InfraRed Thermography

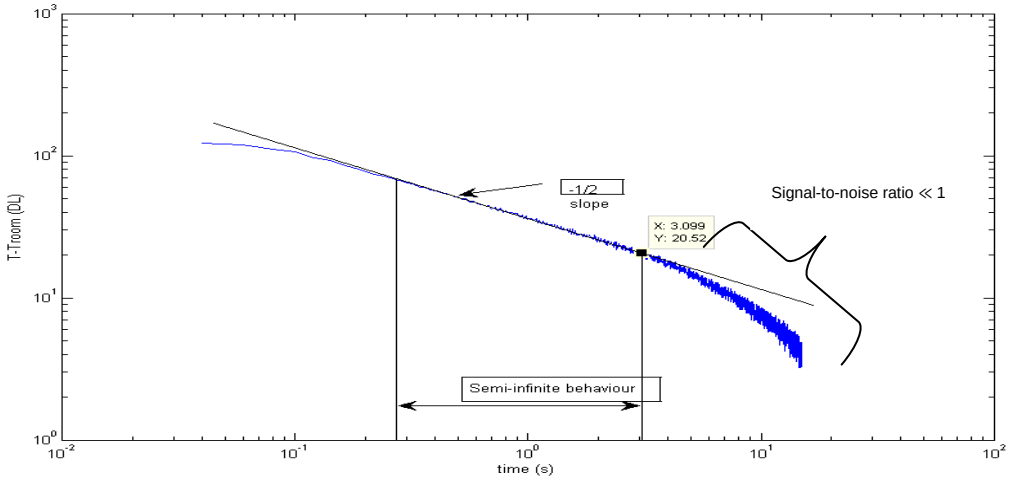

Fig. 4. The logarithm of spatial average value of the temperature ($T-T_{room}$) is plotted versus logaritm of time. T_{room} is the room temperature. The -1/2 slope is well observed until t=3 s, than signal-to-noise ratio is low

3.2 Study of partial spatial average value of temperature in *x* or *y* direction (see (5.b) or (5.c))

The partial spatial average values of temperature, in *x and y* directions, given by expressions (5.b) and (5.c) respectively at *y*=0 and *x*=0 are as follows:

$$\left\langle T(y=0,z=0,t)\right\rangle_x = \frac{Q}{\rho cL}\frac{1}{\sqrt{a_z\pi}}\frac{1}{\sqrt{a_y\pi}}\frac{1}{t} \qquad (6.a)$$

$$\left\langle T(x=0,z=0,t)\right\rangle_y = \frac{Q}{\rho cl}\frac{1}{\sqrt{a_z\pi}}\frac{1}{\sqrt{a_x\pi}}\frac{1}{t} \qquad (6.b)$$

From the previous IR measurements, the logarithm of partial spatial average values of temperature, in *x* and y directions, are plotted versus logarithm of time Fig. 5. The -1 slope is well observed for both cases, which validates expressions (5.b) and (5.c) and also (6.a) and (6.b).

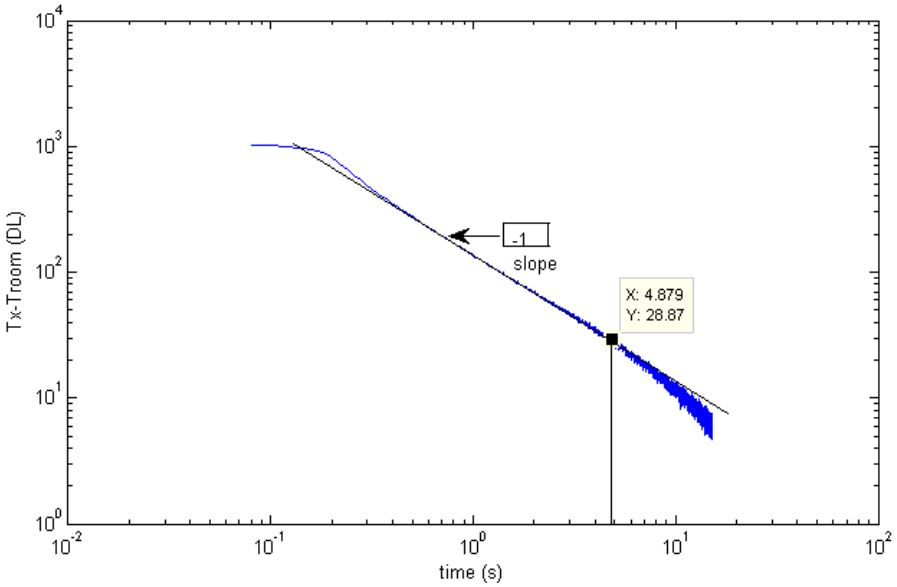

(a)

http://dx.doi.org/10.21611/qirt.2010.009

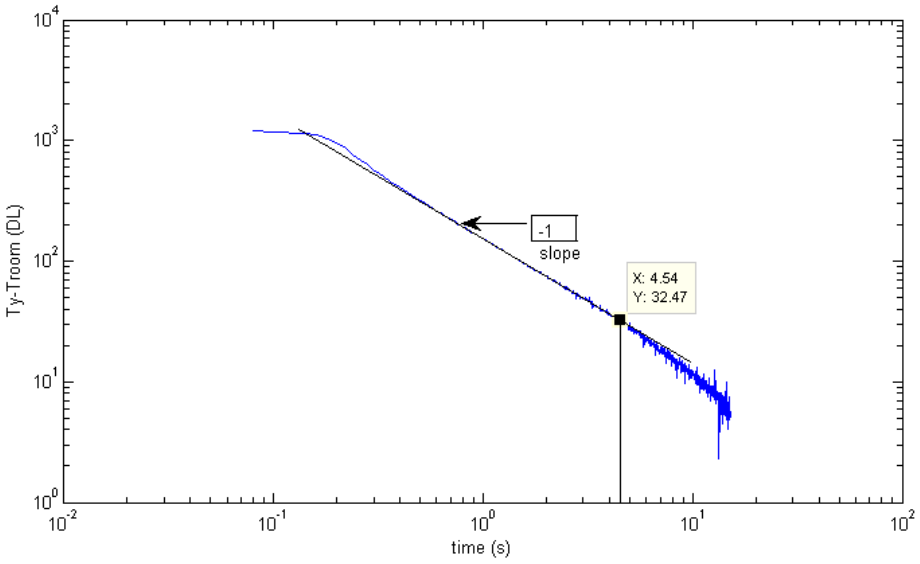

(b)

Fig. 5. (a) The logarithm of partial spatial average value of the temperature *in x direction* (T_x-T_{room}) is plotted versus logaritm of time. The -1 slope is well observed until t=4.9 s, than signal-to-noise ratio is low. (b) The logarithm of partial spatial average value of the temperature *in y direction* (T_y-T_{room}) is plotted versus logaritm of time. The -1 slope is also well observed until t=4.5 s, than signal-to-noise ratio is low

4. Simulation of different diffusion regimes

The 3D analytical expression of the temperature response field of a point source heat pulse, imposed on the front face of a semi-infinite orthotropic solid at *x=y=z=0* yields to equation (1), which is separable and can be expressed as a product of 3 responses related each other to a 1D diffusion behaviour. At z=0, this equation is then:

$$T(x,y,z=0,t)=\frac{Q}{\rho c}\frac{1}{\sqrt{\pi a_z t}}\frac{\exp\left(x^2/(4a_x t)\right)}{\sqrt{\pi a_x t}}\frac{\exp\left(y^2/(4a_y t)\right)}{\sqrt{\pi a_y t}} \quad (7)$$

The last expression (7) is close to 2D analytical expression of the temperature response which is as follows:

$$T(x,y,t)=\frac{Q}{\rho c}\frac{\exp\left(x^2/(4a_x t)\right)}{\sqrt{\pi a_x t}}\frac{\exp\left(y^2/(4a_y t)\right)}{\sqrt{\pi a_y t}} \quad (8)$$

If we now multiply expression (7) by $\sqrt{t}$ then we get:

$$\sqrt{t}\times T(x,y,z=0,t)=\frac{1}{\sqrt{\pi a_z}}\frac{Q}{\rho c}\frac{\exp\left(x^2/(4a_x t)\right)}{\sqrt{\pi a_x t}}\frac{\exp\left(y^2/(4a_y t)\right)}{\sqrt{\pi a_y t}}=\frac{1}{\sqrt{\pi a_z}}T(x,y,t) \quad (9)$$

The 3D response multiplied by $\sqrt{t}$ is equal to 2D response multiplied by the factor $\frac{1}{\sqrt{\pi a_z}}$.

Theoretical simulations (Fig. 6) are performed to show this point. If we multiply expression (5.b) or (5.c) by $\sqrt{t}$, we will get 1D diffusion regime in *y* and *x* directions respectively. This interesting feature, due to separability of analytical solution (1), allows considering different 1D regimes, all obtained from a 3D response *T(x,y,z=0,t)*.

http://dx.doi.org/10.21611/qirt.2010.009
10th International Conference on Quantitative InfraRed Thermography

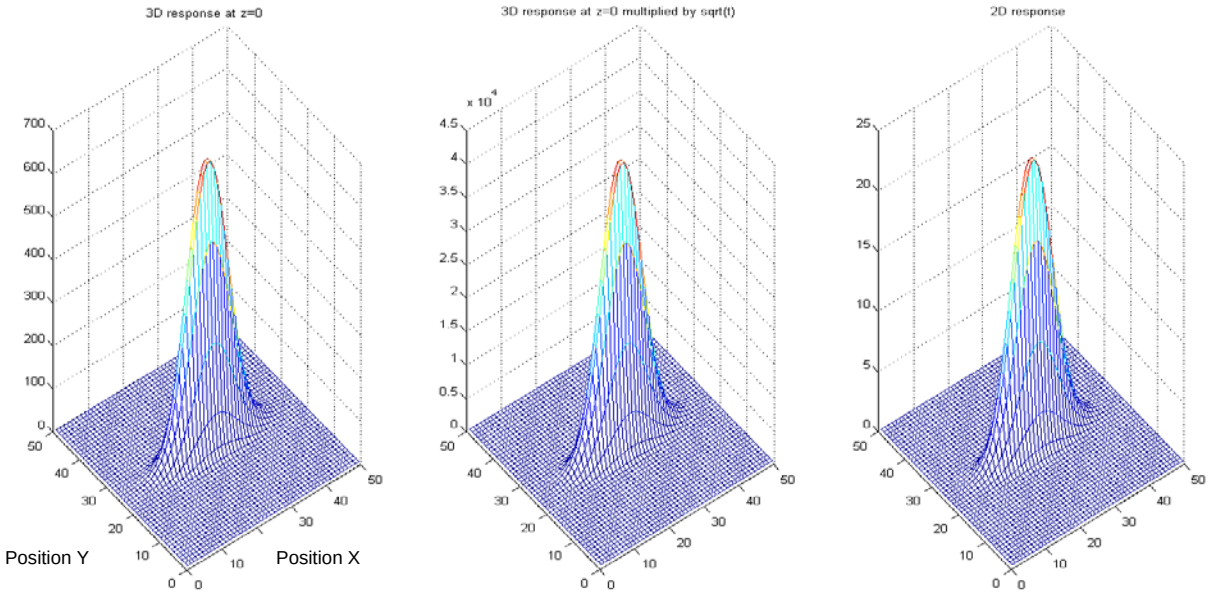

(a) *(b)* *(c)*

Fig. 6. *Instantaneous response of different diffusion regimes after heat pulse. For the simulation we set thermal diffusivities to $a_x=10^{-5}$, $a_y=10^{-6}$, $a_z=10^{-7}$ and $\frac{Q}{\rho c}=1$. We can easily verify that their is a factor $\frac{1}{\sqrt{\pi a_z}}$ between graphs (b) and (c)*

5. Processing of 3D temperature response. Inplane diffusivity estimation

5.1 Inverse processing

From expression (7), $\sqrt{t}\times T(x,y,z=0,t)\propto \tilde{T}(x,y,t)$ verifies a pure inplane diffusion in *x* and *y* directions. In order to estimate the inplane diffusivity it is then suitable to consider the 2D finite differences approximation of heat equation with explicit scheme, by considering the temperature signal $\tilde{T}(x,y,t)=T_{i,j}^{k}$ of one pixel at node *i,j* and at time *k*:

$$Fo_{i,j}\Delta T_{i,j}^{k}=\delta T_{i,j}^{k} \qquad (10)$$

with: $\Delta T_{i,j}^{k}=\left(T_{\mathrm{i+1,j}}^{k}+T_{\mathrm{i-1,j}}^{k}+T_{\mathrm{i,j+1}}^{k}+T_{\mathrm{i,j-1}}^{k}-4T_{i,j}^{k}\right)$ and $\delta T_{i,j}^{k}=T_{i,j}^{k+1}-T_{i,j}^{k}$ the laplacian and the temporal derivative of the temperature, $Fo_{i,j}=\frac{a_{i,j}\Delta t}{\Delta x^{2}}$ is the non-dimensional Fourier local number with: $a_{i,j}$ the local thermal diffusivity (m² s^{-1}), Δx the pixel size (m) with $\Delta x = \Delta y$, Δt the time step (s). The main difficulty consists in finding in the pixels verifying this diffusive model (10).

A simple way to process the temperature response, is to study the correlation coefficient $\rho_{i,j}^{F_t}$ between laplacian and temporal derivative, defined as follows [5]:

$$\rho_{i,j}^{F_t}=\frac{\sum_{F_t}\Delta T_{i,j}^{k}\delta T_{i,j}^{k}}{\sqrt{\sum_{F_t}\Delta T_{i,j}^{k\,2}}\sqrt{\sum_{F_t}\delta T_{i,j}^{k\,2}}} \qquad (11)$$

with F_t a temporal window of length $F_t=\left[k,k+lt\right]$, $k\in[1,N-lt]$, *k* is the time step and *lt* the length of the temporal window.

http://dx.doi.org/10.21611/qirt.2010.009

If such correlation coefficient is near to 1, it is a proof that the purely diffusive model (10) is verified. The inverse thermal Fourier number could be calculated [5] with the formulation:

$$\frac{1}{Fo_{i,j}^{F_t}} = \frac{\sum_{F_t} \Delta T_{i,j}^k \delta T_{i,j}^k}{\sum_{F_t} \delta T_{i,j}^{k\,2}} = \frac{\rho_{i,j}^{F_t} \sqrt{\sum_{F_t} \Delta T_{i,j}^{k\,2}}}{\sqrt{\sum_{F_t} \delta T_{i,j}^{k\,2}}} \quad (12)$$

For the inplane diffusivity estimation with equation (12), we first calculate the correlation equation (11) with a temporal window. When the value of the correlation coefficient is close to 1, we estimate the inverse Fourier number which is related to thermal diffusivity. Otherwise, the estimation is not performed and a zero value is affected to that node. At the end of the process we obtain a global inverse Fourier number by calculating:

$$\frac{1}{Fo_{i,j}^{est}} = \sum_{k=1}^{N-Ft} \frac{1}{Fo_{i,j}^{k}} . \left(\rho_{i,j}^{k} \to 1\right) \Big/ \sum_{k=1}^{N-Ft} \left(\rho_{i,j}^{k} \to 1\right) \quad (13)$$

Then we deduce thermal diffusivity at each node from expression: $Fo_{i,j}^{est} = \frac{a_{i,j} \Delta t}{\Delta x^2}$

5.2 Experimental results

An experimental validation is performed with the previous configuration. The spatial resolution $\Delta x = \Delta y$ obtained with the microscope objective is about 30 µm for each pixel and the acquisition frequency is 50 frames per second (Δt = 20 ms). The number of pixels in the *x* and *y* directions is identical and equals to 200. To decrease the influence of noise and the spatial correlation between pixels, due to the non uniformity correction feature of IR detector, the measured temperature field is averaged by a 4 by 4 square. As a result, the size of the field in *x* and *y* directions is divided by four and the pixel sizes Δx and Δy become equal to 120 µm. The temporal window for calculations is set to F_t =2. The correlation coefficient and inplane diffusivity mappings are represented Fig.7 just after the heat pulse at the time step *t=2s*.

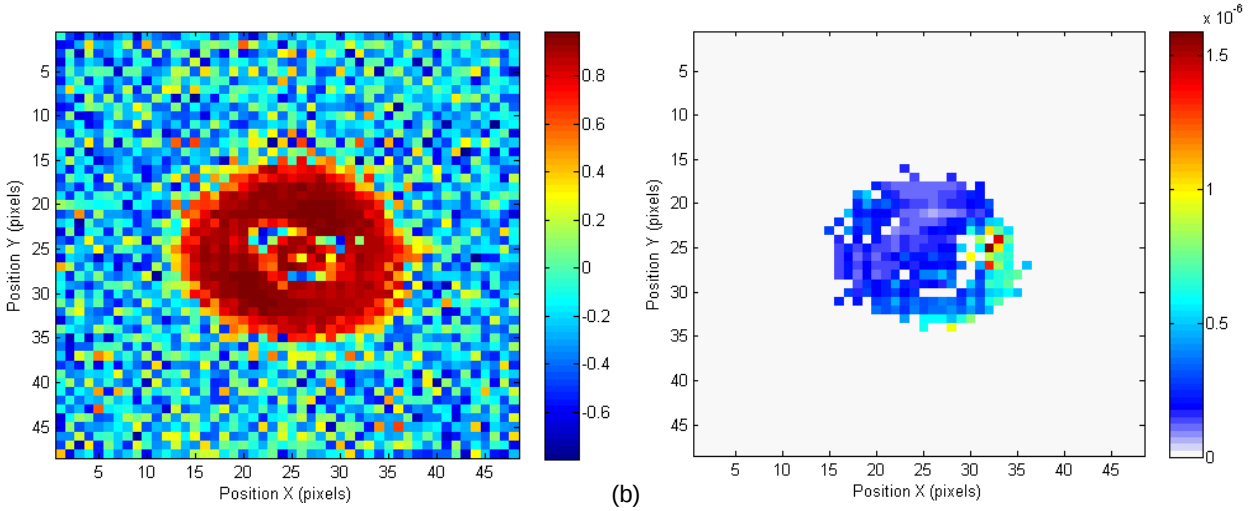

(a) (b)

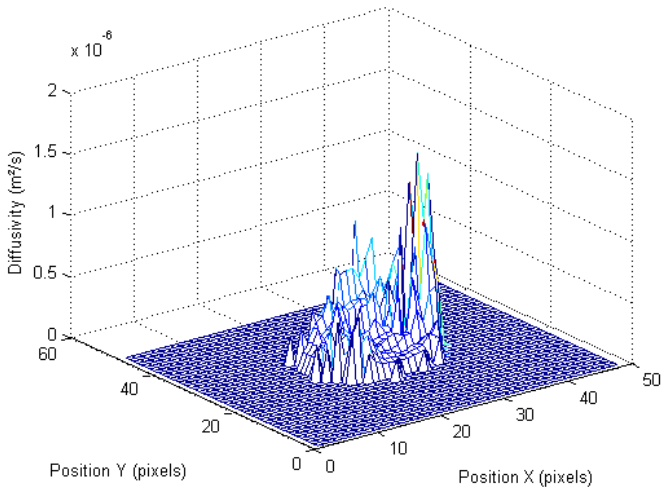

(c)

Fig. 7. *(a) Correlation coefficient mapping of the sample for* F_t =10 at the time step *t=2s (b)-(c) Inplane diffusivity mapping*

The correlation coefficient between laplacian and temporal derivative is close to 1 in the heated area (Fig. 7 (a)). The diffusion model (10) is verified in this zone. The local diffusivities could then be estimated (Fig. 7 (b)-(c)). Outside this area the signal-to-noise ratio is low, the correlation coefficient $\rho_{i,j}^{k} << 1$. The local diffusivities could not be estimated.

6. Conclusion. Perspectives

The results presented in this paper are a preliminary step in order to validate the point source method and to show different processing possibilities with IR cameras.

The perspectives of the use of the point source are for example to exploit the possibilities of superposition of such sources by a space shift of the laser. One way to study very short times will be also explored with heterodyne methods [6].

REFERENCES

[1] CARLSLAW H.S., JAEGER J.-C., "Conduction of Heat in solids", Oxford, Clarendon Press, 1959

[2] GUSTAFSON SE., "Transient plane source techniques for thermal conductivity and thermal diffusivity measurements of solid materials", Rev. Of Sci. Instrum., Vol. 62, 797, 1991

[3] PHILIPPI I., BATSALE J.-C., MAILLET D., DEGIOVANNI A., "Measurement of thermal diffusivity trough processing of infrared images", Rev. Sci. Instrum., 66, pp182-192, 1995

[4] KRAPEZ J.C., SPAGNOLO L., FRIEB M., MAIER H.P. NETTER F., "Measurement of in-plane diffusivity in non-homogeneous slabs by applying flash thermography", International Journal of Thermal Sciences 43 967-977, 2004.

[5] PRADÈRE C., MORIKAWA J., TOUTAIN J., BATSALE J.-C., HAYAKAWA E., HASHIMOTO T., "Microscale thermography of freezing biological cells in view of cryopreservation", QIRT Journal, Vol. 6., No. 1, pp. 37-61, 2006

[6] CLERJAUD L., PRADÈRE C., BATSALE J.-C., DILHAIRE S., "Heterodyne method: thermal diffusivity estimation with periodic local heating in a large range of frequencies (25 Hz to upper than 1 kHz)", QIRT Journal, Vol. 7., No. 1, pp. XX-XX, 2010 (in press)